Interference of Spinodal Waves in Thin Polymer Films

Georg Krausch,*,†,‡ Chi-An Dai,†,‡ Edward J. Kramer,*,†,‡ and John F. Marko‡,§

Department of Materials Science and Engineering, Materials Science Center, and Laboratory of Atomic and Solid State Physics, Cornell University, Ithaca, New York 14853-1501

Frank S. Bates

Department of Chemical Engineering and Materials Science, University of Minnesota, Minneapolis, Minnesota 55455

Received May 5, 1993; Revised Manuscript Received June 17, 1993®

ABSTRACT: We have studied the thickness dependence of the spinodal decomposition in thin films of a binary polymeric mixture. Nuclear reaction analysis (NRA) and time-of-flight forward recoil spectrometry (TOF-FRES) have been used to monitor the phase separation in thin films of poly(ethylenepropylene) (PEP) and perdeuterated poly(ethylenepropylene) (dPEP) after a quench into the two-phase region. The composition profiles are modeled by two distinct spinodal waves originating from the two surfaces of the films, and interference effects are observed as the film thickness is varied. Below a critical film thickness the coarsening of the phase structure is found to be severely altered with respect to the thick film behavior. Cell-dynamical simulations have been performed which closely resemble the experimental findings.

The spinodal decomposition of binary mixtures has been a matter of considerable interest in the past, both experimentally and theoretically.[1-5] Following a rapid quench from the one-phase region into their miscibility gap, bulk fluids phase separate through an exponential growth of concentration fluctuations with a characteristic, time-independent wavenumber q_m. At later times, the wavenumber shifts toward zero, leading to an increasingly coarsened phase structure. This process is characterized by an isotropic structure factor, reflecting the translational and rotational symmetry of the bulk fluid. However, a quite different behavior can be expected when the symmetry is broken, e.g., in the vicinity of a surface.[6-9] This has first been suggested by Ball and Essery on theoretical grounds[6] and was confirmed shortly after by Jones et al.,[10] who observed a strongly anisotropic structure factor in the spinodal decomposition of thin films of an isotopic polymer blend. The film surface was found to be enriched in one of the components, and an oscillatory composition profile was observed perpendicular to the surface. The characteristic wavelength of this layered structure was found to grow considerably slower with respect to the bulk behavior.[11] In a similar kind of experiment, Bruder and Brenn concentrated on the equilibrium phase structure at late times;[12] they could show that a stable layered structure of binodal compositions can only be established when both interfaces are completely wet by one of the components. Otherwise, the competing growth of bulk domains was found to eventually destroy the layered structure.

In the present study, we shall investigate the influence of the film thickness on the spinodal decomposition of a binary polymer mixture. Assuming an attraction of either of the two components to both the polymer/vacuum and the polymer/substrate interfaces, respectively, one expects two separate spinodal waves to extend into the film which eventually will interact with each other as the film thickness becomes comparable to the decay length of the oscillations. We present the first experimental evidence for both constructive and destructive interference of these waves by varying the film thickness. In addition we show that the coarsening of the spinodal wave is considerably slowed down as the film thickness becomes smaller than some critical value. Finally, the experimental findings will be shown to be in good agreement with cell-dynamical simulations based on a modified time-dependent Ginzburg-Landau model[13] of phase ordering including symmetry-breaking surface fields.[7]

The system under consideration is a symmetric binary mixture of poly(ethylenepropylene) (PEP) and perdeuterated poly(ethylenepropylene) (dPEP) with approximately equal index of polymerization $N_H = N_D = N = 2286$. The polymers were synthesized following standard methods.[14] The mixture is characterized by a small, positive interaction parameter χ, resulting from the slight differences in bond length and polarizability between the C-H and the C-D bonds,[15,16] respectively. This in turn leads to an upper critical solution temperature $T_c = 365$ K, below which phase separation occurs. In addition, the deuterated component is found to have a somewhat smaller surface energy and tends to segregate to the film surface.[17]

Thin PEP/dPEP films with nearly critical concentration $\Phi \approx 0.50$ were prepared by spin casting. Toluene solutions of varying concentration were spread onto a Si wafer; the native SiO_2 surface layer was removed by etching in aqueous HF immediately prior to film deposition ("stripping"). Film thicknesses ranged between 150 and 1000 nm. The samples were then annealed under vacuum at 321 K for various times. Since the glass transition of PEP is well below room temperature ($T_g = 217$ K), the samples were analyzed immediately after annealing if possible or else stored in liquid nitrogen in order to prevent any further, uncontrolled phase separation from occurring at room temperature.

The volume fractions of the two components were determined as a function of depth perpendicular to the film surface by either nuclear reaction analysis (NRA) or time-of-flight forward recoil spectrometry (TOF-FRES).

* To whom correspondence should be addressed. Present address for G.K.: Fakultät für Physik, Universität Konstanz, Postfach 5560, D-78434 Konstanz, FRG.
† Department of Materials Science and Engineering.
‡ Materials Science Center.
§ Laboratory of Atomic and Solid State Physics.
® Abstract published in *Advance ACS Abstracts*, September 15, 1993.

0024-9297/93/2226-5566$04.00/0

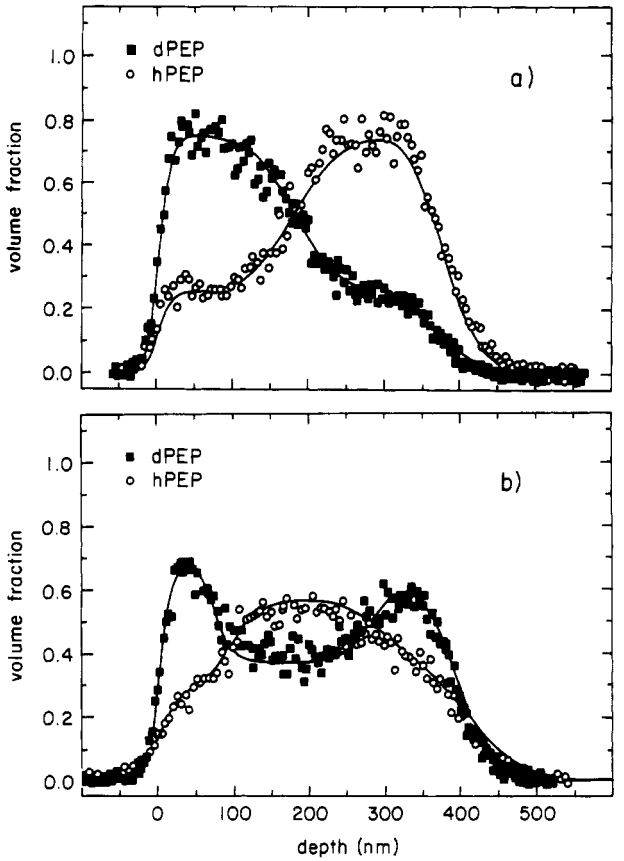

Figure 1. Volume fraction vs depth profiles for both dPEP (open squares) and hPEP (open circles) as determined by TOF-FRES. The films were annealed for 116 h at 321 K. (a) Stripped Si substrate; (b) Si substrate covered a self-assembled methyl-terminated organic monolayer produced by treating the Si with OTS prior to film deposition. The solid lines are guides to the eye.

NRA takes advantage of the exothermic nuclear reaction $^3He(^2H,^1H)^4He$ and therefore is sensitive to the deuterated component only. TOF-FRES, on the other hand, probes both hydrogen and deuterium through elastic scattering, with however a somewhat poorer depth resolution. While both techniques were used in a complementary manner, a complete set of data was always taken with the same technique to avoid any systematic errors. (For details concerning the techniques and their particular application to isotopic polymer mixtures, refer to refs 18 and 19, respectively).

We shall first address the question of which of the two components of the mixture will preferably segregate to the Si substrate surface. Similar to the results of Bruder and Brenn,[12] the behavior of the PEP/dPEP mixture in the vicinity of the substrate is found to strongly depend on the history of this surface and may easily be changed by varying the substrate surface energy. A detailed study of this effect will be the subject of a forthcoming publication; however, to clarify the situation faced in the present study, Figure 1 shows volume fraction vs depth profiles for an initially uniform critical mixture after annealing for 116 h at 321 K on two different substrate surfaces. While Figure 1a shows the results for a polymer film spun directly onto a stripped Si surface, Figure 1b shows the results for a polymer film spun similarly onto a self-assembled monolayer of octadecyltrichlorosilane (OTS), which was grafted onto the Si surface prior to film deposition. As can be clearly seen from Figure 1a, the quench into the two-phase region finally leads to the formation of a bilayer structure with a dPEP-rich component close to the polymer/vacuum interface and an PEP-rich component close to the stripped Si surface. The introduction of a self-assembled monolayer, on the other hand, leads to a quite different phase morphology now characterized by a dPEP-rich phase close to both the film surface and the film/substrate interface. We include this information to emphasize the importance of the polymer/substrate interface for the overall film morphology. However, the remainder of the paper shall be solely concerned with polymer films on stripped Si substrates.

It is tempting to compare the observed plateau values of the respective volume fractions in Figure 1a with the binodal concentrations expected from a Flory–Huggins mean-field theory. Only recently, Gehlsen et al. reported a comprehensive study of the effective Flory–Huggins interaction parameter χ_{eff} as a function of temperature, molecular weight, and relative deuterium content in PEP/dPEP mixtures.[16] For our polymers $\chi_{eff} = 1.08\ (6) \times 10^{-3}$ at 321 K from these data; using this we arrive at binodal concentrations of $\Phi_1 = 0.16$ and $\Phi_2 = 0.84$. The observed values do not match the theoretical predictions but are well inside these (e.g., $\Phi_1 = 0.25$ and $\Phi_2 = 0.75$ from Figure 1a). It may be that longer annealing times are needed to completely equilibrate the system, but additional experiments clearly show that the layered structure is stable over times longer than several years. We shall only conclude at this point that the stripped silicon surface attracts the hydrogenated rather than the deuterated component of the mixture. This fact shall be of importance for the following considerations.

In order to study the interaction of the spinodal waves originating from the two surfaces confining the films, we shall now turn to considerably shorter annealing times where the spinodal waves can be expected to extend into only a portion of the film thickness. The proper annealing times were chosen so as to match the accessible depth resolution and depth range of the profiling techniques. Figure 2 shows concentration vs depth profiles $\Phi_{dPEP}(z)$ of the deuterated component for various film thicknesses after annealing for 5.5 h at 321 K. If we start from very thick films (Figure 2a), only the surface spinodal wave can be observed, decaying into the bulk of the films over a characteristic length of some 250 nm. No oscillations originating from the Si surface are observed as the back part of the film lies well beyond the accessible depth range of NRA. The data are well represented by

$$\Phi_{dPEP} = 0.5 + \Phi_{dPEP;surf} \tag{1}$$

with

$$\Phi_{dPEP;surf} = \frac{\Phi_{dPEP;0}}{(2\pi\sigma^2)^{1/2}} \exp\left(-\frac{z}{2\sigma}\right)^2 \cos(q_m z) \tag{2}$$

where $\Phi_{dPEP;surf}$ is a damped cosine oscillating about the average concentration $\Phi_c = 0.5$. In order to correct for the finite experimental depth resolution, this function was then convoluted with a Gaussian with a depth-dependent width ranging from about 20 nm at the film surface to about 100 nm at a depth of 600 nm.[20] The best fit to the experimental data was achieved for a characteristic wave vector $q_m = 2.56\ (10) \times 10^{-3}$ Å^{-1} and a decay length $\sigma =$ 230 (15) nm. The dPEP volume fraction at the film surface was found to amount to 0.85 corresponding to an amplitude $\Phi_{dPEP;0} = 0.35$.

As the film thickness d is decreased, the observed composition profile changes markedly. As can be seen in Figure 2b, a third maximum of the composition wave is found at around 500 nm. This maximum is due to a second spinodal wave, originating the polymer/substrate interface.

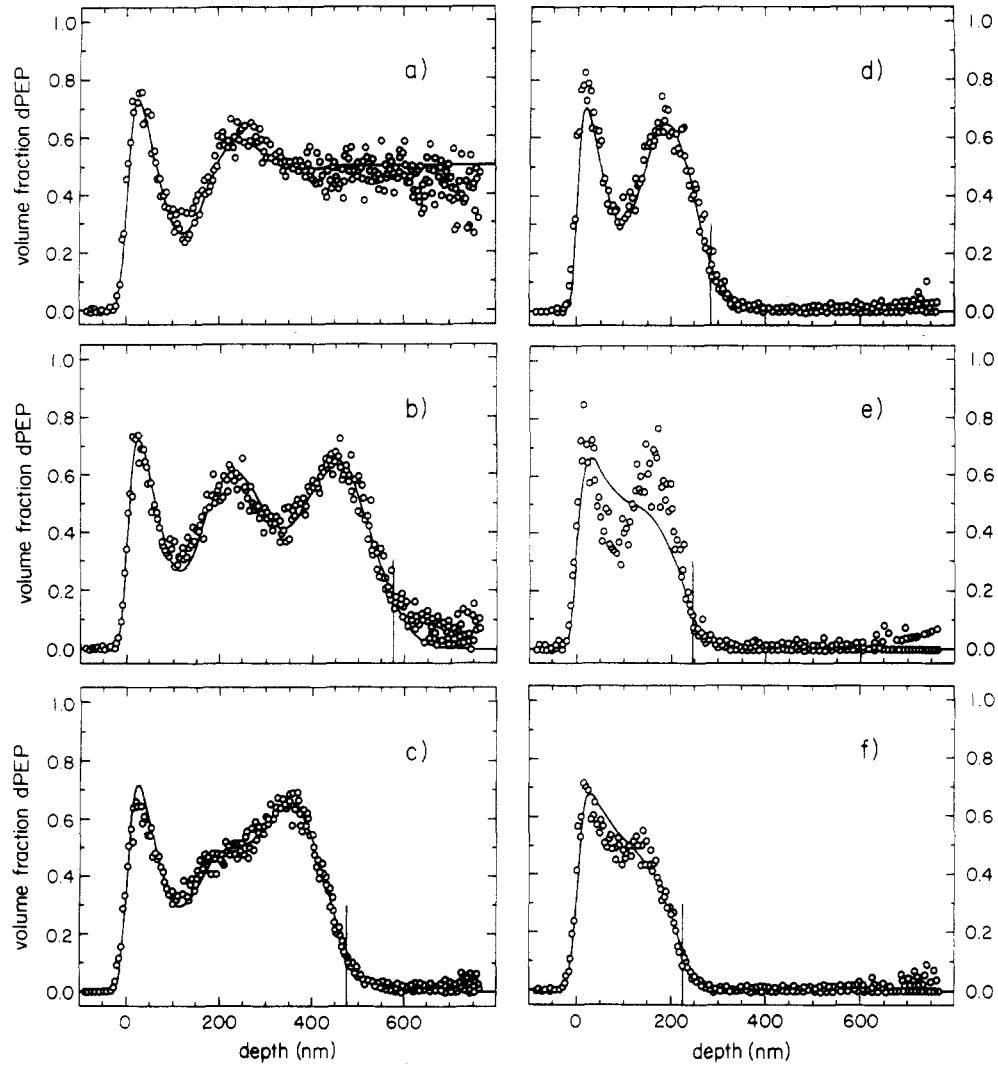

Figure 2. dPEP volume fraction vs depth profiles for different film thicknesses d as determined by NRA: (a) $d > 1000$ nm, (b) $d = 574$ nm, (c) $d = 474$ nm, (d) $d = 282$ nm, (e) $d = 240$ nm, (f) $d = 220$ nm. The solid lines represent the result of eq 3 convoluted with a Gaussian of increasing full width at half-maximum. The locations of the Si substrates are indicated by the vertical lines. (All substrates were stripped from oxide prior to film deposition.)

In order to fit the data, we therefore add a second wave to eq 1

$$\Phi_{dPEP} = 0.5 + \Phi_{dPEP;surf} + \Phi_{dPEP;subs} \quad (3)$$

with

$$\Phi_{dPEP;subs} = -\frac{\Phi_{hPEP;0}}{(2\pi\sigma^2)^{1/2}} \exp(-(z/2\sigma)^2) \cos(q_m(d-z)) \quad (4)$$

the negative sign being due to the fact that the hydrogenated rather than the deuterated component of the mixture is attracted to the Si surface as discussed above. While it seems reasonable to assume that both q_m and σ mainly reflect bulk properties and therefore should be independent of the particular surface the spinodal wave originates from, it is by no means obvious that the amplitude of the oscillation is the same for both interfaces. Lacking further information on the strength of the substrate polymer interaction, we take $\Phi_{hPEP;0} = \Phi_{dPEP;0} = 0.35$ for a first trial. As can be seen in Figure 2b, eq 4 fits the experimental data quite well, with the film thickness d being the only adjustable parameter during the fit. We shall point out, however, that, due to the limited depth resolution at the back interface of the film, the value of $\phi_{hPEP;0}$ can only be estimated roughly.

If the above model were correct, one should be able to observe interference of the two spinodal waves as the film thickness is further decreased and major parts of the waves can interact with each other. This is indeed the case and can be seen in parts c and d of Figure 2, where we first find complete destruction of the second maximum followed by constructive interference as the film thickness is decreased. The data are still well represented by eq 3 with all parameters but the film thickness kept at their initial values.

Marked changes in the fit are observed, however, when the film thickness is further decreased. These can be seen in parts e and f of Figure 2, where the theoretical profiles according to eq 3 clearly fail to predict the experimental data. This discrepancy is observed in all samples thinner than about 280 nm. In order to still represent the data in Figure 2e with eq 3, we have to decrease the characteristic wave length of the oscillations markedly. To understand this effect, we may compare the total film thickness to the most probable wavelength at early times. As the wave vectors of the surface spinodal waves approach the bulk value at $t = 0$, we may extrapolate the data for $q_{m,bulk}$ obtained from light scattering experiments on bulk PEP/dPEP samples[21] to $t = 0$. We estimate $q_{m,bulk}(t=0) = 3.6 \times 10^{-3}$ Å^{-1} for $T = 321$ K, corresponding to $\lambda_m(t=0) = 174$ nm. Since the substrate surface is covered by a PEP-rich layer in contrast to the polymer/vacuum interface, a minimal film thickness of $d_{min} = 1.5\lambda_m(t=0) = 261$ nm is

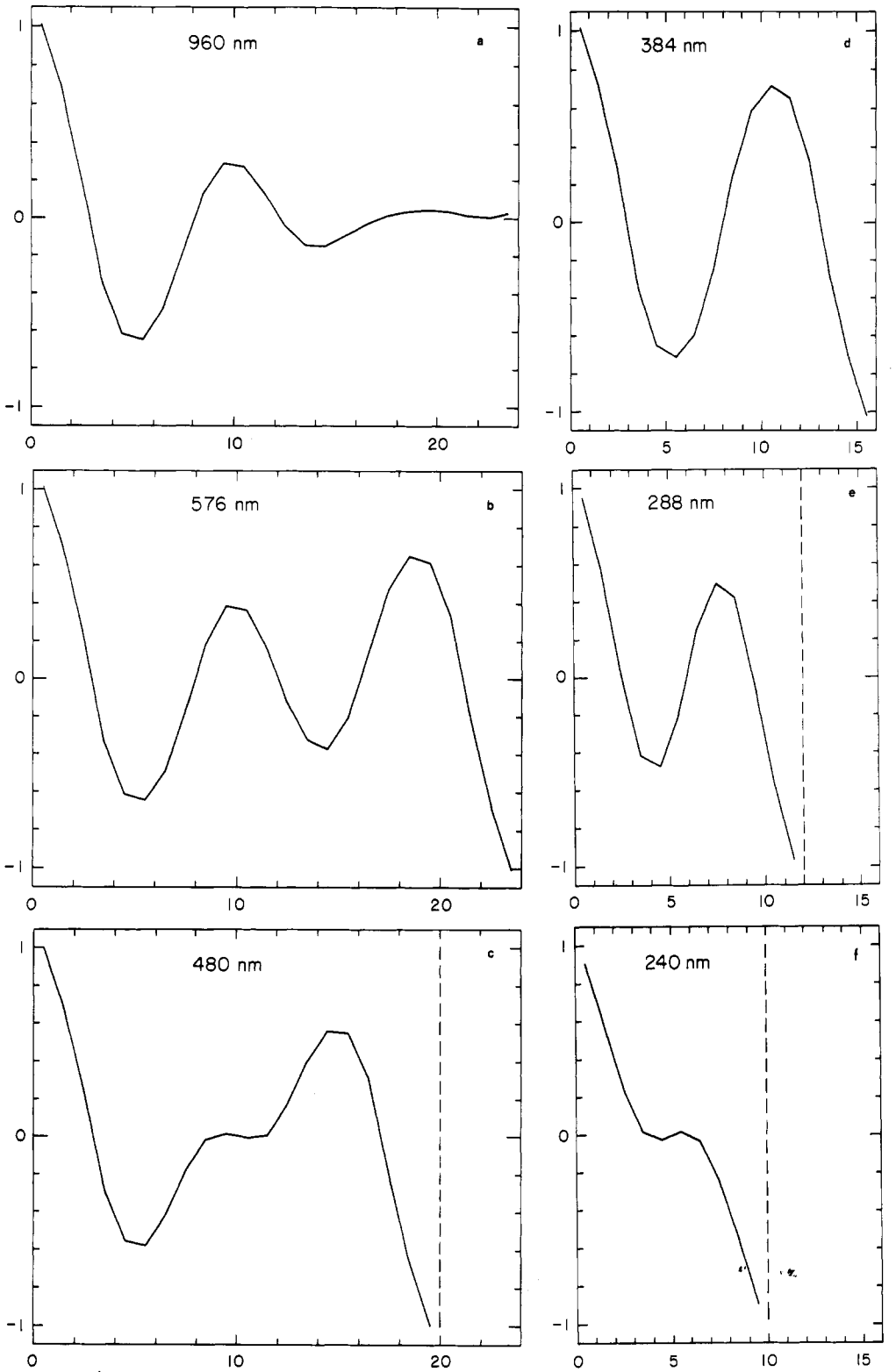

Figure 3. Results of the cell-dynamical simulations after 304 time steps (≈5.8 h) for different film thicknesses closely resembling the experimental situation shown in Figure 2: (a) 960 nm, (b) 576 nm, (c) 480 nm, (d) 384 nm, (e) 288 nm, and (f) 240 nm. The solid lines show the order parameter Ψ, averaged over the xy plane as a function of depth beneath the surface (given in numbers of cells).

needed in order to realize a composition wave with $q_{m,bulk}$-(t=0). As the film thickness falls below this limit, the system is forced to decompose with a larger characteristic wave vector, which then is determined by the macroscopic dimensions of the film. A detailed study of this thickness regime is beyond the scope of this paper; yet, interesting effects can be expected with respect to both the nonequilibrium and the final equilibrium phase structure of such ultrathin film systems.

In order to compare the above findings to recent theoretical studies, we have performed cell-dynamical simulations based on an extended conserved time-dependent Ginzburg–Landau (CTDGL) model,[7] which is the Cahn–Hilliard–Cook model including surface interactions and nonlinearities. We start from a free energy functional[22]

$$\frac{F}{kT} = \mathrm{d}^3\mathbf{r}\left\{\frac{\epsilon}{2}\Psi^2 + \frac{u}{4}\Psi^4 + \frac{c}{2}(\nabla\Psi)^2 - \left(\sigma_1\Psi + \frac{\sigma_2}{2}\Psi^2\right)\delta(z)\right\} \tag{5}$$

where the order parameter $\Psi(\mathbf{r},t)$ represents the difference between the local concentrations of the two pure com-

ponents and σ_1 and σ_2 are surface potentials. The CTDGL equation of motion[13] takes the form of a conservation law for the order parameter $\Psi(\mathbf{r},t)$:

$$\frac{\partial\Psi(\mathbf{r},t)}{\partial t} = \nabla\{M\nabla\mu(\mathbf{r},t) + \mathbf{j}(\mathbf{r},t)\} \tag{6}$$

where M is a constant mobility and the noise current $\mathbf{j}$ is required to finally drive the field to thermal equilibrium. $\mathbf{j}$ has correlations

$$\langle j_\alpha(\mathbf{r},t)\, j_\beta(\mathbf{r}',t')\rangle = 2MkT\delta_{\alpha\beta}\delta^3(\mathbf{r}-\mathbf{r}')\,\delta(t-t') \tag{7}$$

The chemical potential $\mu = \delta F/\delta\Psi$ is the functional derivative of the free energy F with respect to Ψ. We assume that the system is in the one-phase region at times $t < 0$ and study the behavior of the order parameter after a quench below the critical temperature at $t = 0$. With $\epsilon = a_0$ for $t < 0$ and $\epsilon = -a$ for $t > 0$, we can rescale the above model using the characteristic times, distances, and field strengths of the $t > 0$ dynamics. We use the scaling transformations $\mathbf{r}/(c/a)^{1/2} \rightarrow \mathbf{r}$, $t/(c/Ma^2kT) \rightarrow t$, and $\Psi/(a/u)^{1/2} \rightarrow \Psi$ to obtain

$$\frac{\partial\Psi(\mathbf{r},t)}{\partial t} = \nabla^2\{\tau\Psi(\mathbf{r},t) + \Psi^3(\mathbf{r},t) - \nabla^2\Psi(\mathbf{r},t)\} + g^{1/2}\eta(\mathbf{r},t) \tag{8}$$

with $\tau = a_0/a$ for $t < 0$ and $\tau = -1$ for $t > 0$, and $g = 2ua^{-1/2}c^{-3/2}$. The scalar noise $\eta(\mathbf{r},t)$ has correlations $\langle\eta(\mathbf{r},t)\,\eta(\mathbf{r}',t')\rangle = -\nabla^2\delta^3(\mathbf{r}-\mathbf{r}')\,\delta(t-t')$. The rescaled surface potentials $s_1 = a^{-1}(u/c)^{1/2}\sigma_1$ and $s_2 = a^{-1/2}c^{-1/2}\sigma_2$ enter through the boundary condition[7]

$$0 = \mathbf{z}\cdot\nabla\Psi + s_1 + s_2\Psi \tag{9}$$

$\mathbf{z}$ being the unit vector perpendicular to the surface. In addition, we choose boundary conditions $\mathbf{z}\cdot\nabla\mu = \mathbf{z}\cdot\mathbf{j} = 0$ so that there is no flux of the order parameter across the boundary surface. To study the dynamics of eq 8, we have used three-dimensional cell-dynamical systems,[23] which may be roughly considered as a discretization of time and space. Periodic boundary conditions are used in the x and y directions, and the z dimension is limited by two impenetrable surfaces with surface potentials of equal strength but opposite sign. Details of the cell-dynamical simulations (CDS) are given in ref 7. Using a statistical segment length $b = 0.8$ nm for PEP as well as the data for N and T_c specified above, we calculate the parameters a, c, and u[22] and estimate the length $(c/a)^{1/2}$ to be 19.6 nm. In the CDS, the lattice spacing is 1.24 of this length, i.e., 24 nm. Taking the mutual diffusion coefficient to be D(321 K) = 7×10^{-15} cm^2/s,[21] the time $\{c/Ma^2kT\}$ corresponds to be about 550 s. Again, in the CDS one time step corresponds to 0.126 of this unit time, i.e., 69 s. We further estimate $kT\sigma_1 = 0.1$ mJ/m^2 and $kT\sigma_2 = -0.01$ mJ/m^2 from the surface energy difference between the two isotopic polymer species.[24]

In order to compare to the experimental situation, Figure 3 shows the order parameter Ψ, at 304 time steps (≈5.8 h) after the quench averaged over the xy plane for different numbers of cells in the z direction.[25] Qualitatively, the data clearly resemble the experimental results shown in Figure 2; this conclusion holds both for the observation of destructive and constructive interference of the two waves and for the fact that the characteristic wavelength λ_m is found to be independent of the film thickness in the case of sufficiently thick films. This independence is seen from the fact that the first minimum stays at approximately the same depth for all simulations down to a thickness of 16 cells. In addition, a change of the characteristic wavelength is observed as the film thickness

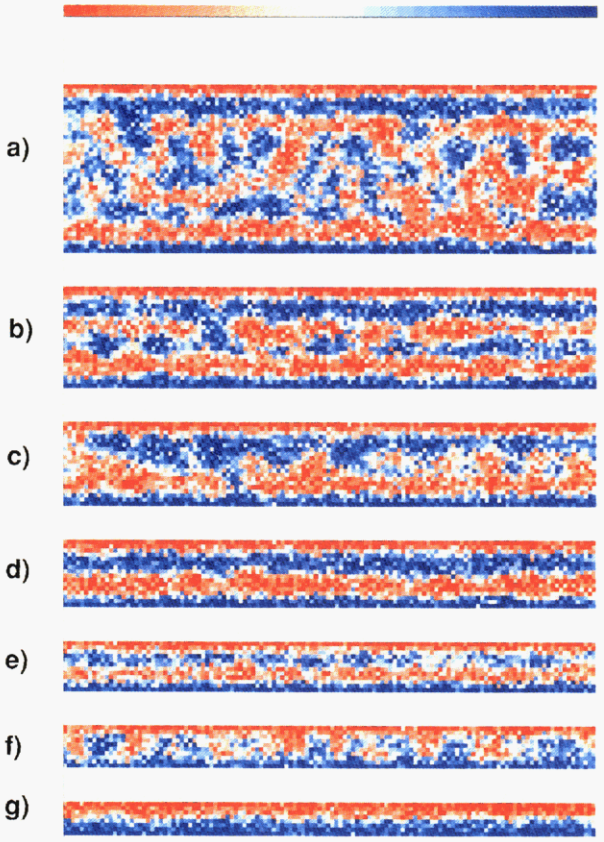

Figure 4. Value of the order parameter Ψ in a plane perpendicular to the film surface after 304 time steps (≈5.8 h). The films thicknesses are the same as in Figure 3: (a) 40 cells, (b) 24 cells, (c) 20 cells, (d) 16 cells, (e) 12 cells, (f) 10 cells, and, in addition, (g) 8 cells. The color scale ranges from blue ($\Psi = 1$) to red ($\Psi = -1$).

is further decreased to 12 cells. Similar to the experimental finding, this effect occurs when the film thickness falls below about 1.5 times the characteristic wavelength of the thick film regime, i.e., about $1.5 \times 10 = 15$ cells.[26]

Comparing the above results quantitatively, we may estimate $\lambda_{m,sim} = (10)(1.24)(c/a)^{1/2} = 243$ nm for the thick film regime (Figure 3a–c) and relate this number to the experimental value $\lambda_{m,exp} = 245$ nm. Keeping in mind that no adjustable parameters enter into the simulation and regarding the uncertainties buried in the estimates of both the diffusion coefficient and the surface fields, this agreement is good.

Finally, we shall investigate the lateral phase morphology related to what occurs as constructive and destructive interference of the spinodal waves perpendicular to the confining surfaces. Due to the inherent averaging of the profiling techniques, this information is not accessible in our experiments. We can however extract some information from the cell-dynamical simulations by plotting zx or zy planes of the cell assembly rather than averaging over both x and y. Such plots are shown in Figure 4 where we plot the value of $\Psi(x_0,y,z,t_0)$ for an arbitrarily chosen yz plane for different film thicknesses. The figure clearly shows that "destructive interference" of the spinodal wave corresponds to the existence of a region close to the center of the film consisting of a large number of droplets of either of the two phases. This occurs in parts c and e of Figure 4 and can be understood as the compromising reaction of the system to competing surface fields which tend to enrich the particularly layer by one and the other phase at the same time. The resulting disorder disappears

as soon as the film thickness approaches a value where both surface fields favor the same phase to be enriched at any given plane in the film (Figure 4d). "Constructive interference" therefore corresponds to an almost perfectly layered structure.

In conclusion, we have studied the thickness dependence of the anisotropic spinodal decomposition of thin polymer films. Evidence was given that two distinct spinodal waves originate from the two surfaces of the film at early times that interact with each other as the film thickness becomes comparable to the decay length of the waves. Constructive and destructive interferences were observed and could be modeled by the superposition of two damped oscillatory waves. This picture was shown to break down as the film thickness becomes smaller than the characteristic wavelength for bulk spinodal decomposition at early times. The observed behavior could be resembled by cell-dynamical simulations on the basis of the conserved time-dependent Ginzburg–Landau theory.

Acknowledgment. This work was supported by the NSF-DMR Polymer Program Grant No. DMR-8719123. G.K. greatly appreciates financial support through the Max-Kade-Foundation, New York. J.F.M. was supported by the MRL program of the NSF under Award No. DMR-91216454. F.S.B. is indebted to the NSF for support through Grant No. DMR-8957386. The authors are indebted to R. Sharma and M. Calistri-Yeh for their help preparing the OTS layers. We thank M. H. Rafailovich, J. Sokolov, L. J. Norton, and A. Chakrabarti for useful discussions. The skillful help of N. Szabo and P. Revesz during the course of the experiments is gratefully acknowledged.

References and Notes

(1) de Gennes, P.-G. *Scaling Concepts in Polymer Physics*; Cornell University Press: London, 1979.
(2) Bates, F. S.; Wiltzius, P.; Heffner, W. R. *Phys. Rev. Lett.* **1988**, *60*, 1538. Bates, F. S.; Wiltzius, P. *J. Chem. Phys.* **1990**, *91*, 3258.
(3) de Gennes, P.-G. *J. Chem. Phys.* **1980**, *72*, 4756.
(4) Pincus, P. *J. Chem. Phys.* **1981**, *75*, 1986.
(5) Binder, K. *J. Chem. Phys.* **1983**, *79*, 6387.
(6) Ball, R. C.; Essery, R. L. H. *J. Phys. Condens. Matter* **1990**, *2*, 10303.
(7) Marko, J. F. *Phys. Rev. A*, submitted.
(8) Brown, G.; Chakrabarti, A. *Phys. Rev. A* **1992**, *46*, 4829.
(9) Puri, S.; Binder, K. *Phys. Rev. A* **1992**, *46*, R4487.
(10) Jones, R. A. L.; Norton, L. J.; Kramer, E. J.; Bates, F. S.; Wiltzius, P. *Phys. Rev. Lett.* **1991**, *66*, 1326.
(11) For the time dependence of the growth of surface domains, see also: Wiltzius, P.; Cumming, A. *Phys. Rev. Lett.* **1991**, *66*, 3000.
(12) Bruder, F.; Brenn, R. *Phys. Rev. Lett.* **1992**, *69*, 624.
(13) Gunton, J. D.; San Miguel, M.; Sahni, P. S. In *Phase Transitions and Critical Phenomena*; Domb, C., Lebowitz, J., Academic Press: London, 1983; Vol. 8.
(14) Bates, F. S.; Rosedale, J. H.; Bair, H. E., Russell, T. P. *Macromolecules* **1988**, *21*, 86.
(15) Bates, F. S.; Wignall, G. D.; Koehler, W. C. *Phys. Rev. Lett.* **1985**, *55*, 2425.
(16) Gehlsen, M. D.; Rosedale, J. H.; Bates, F. S.; Wignall, G. D.; Hansen, L.; Almdal, K. *Phys. Rev. Lett.* **1992**, *68*, 2452.
(17) Jones, R. A. L.; Kramer, E. J.; Rafailovich, M. H.; Sokolov, J.; Schwarz, S. A. *Phys. Rev. Lett.* **1989**, *62*, 280.
(18) Chaturvedi, U. K.; Steiner, U.; Zak, O.; Krausch, G.; Schatz, G.; Klein, J. *Appl. Phys. Lett.* **1990**, *56*, 1228.
(19) Sokolov, J.; Rafailovich, M. H.; Jones, R. A. L.; Kramer, E. J. *Appl. Phys. Lett.* **1989**, *54*, 590.
(20) The depth dependence of the spatial resolution of the two profiling techniques has been determined in a separate set of experiments on thin films of stable isotopic polymer mixtures of varying thickness.
(21) Kredowski, C.; Bates, F.; Wiltzius, P. *Macromolecules* **1993**, *26*, 3448.
(22) For a polymer melt, we take $\epsilon = 6(1 - T/T_c)/Nb^3$, $c = 1/b$, and $u = 1/Nb^3$, with N being the index of polymerization, b the statistical segment length, and T_c the critical temperature in K.
(23) Oono, Y.; Puri, S. *Phys. Rev. Lett.* **1987**, *58*, 836. Oono, Y.; Puri, S. *Phys. Rev. A* **1988**, *38*, 434. Oono, Y.; Puri, S. *Phys. Rev. A* **1988**, *38*, 1542. Shinozaki, A.; Oono, Y. *Phys. Rev. Lett.* **1991**, *66*, 17323.
(24) Norton, L., unpublished.
(25) An anneal at $T = 409$ K was carried out in the CDS before quenching.
(26) We may take the approximate position of the first minima of the solid lines in Figure 3 as a measure of half the characteristic wavelength.